Timeline of the Universe

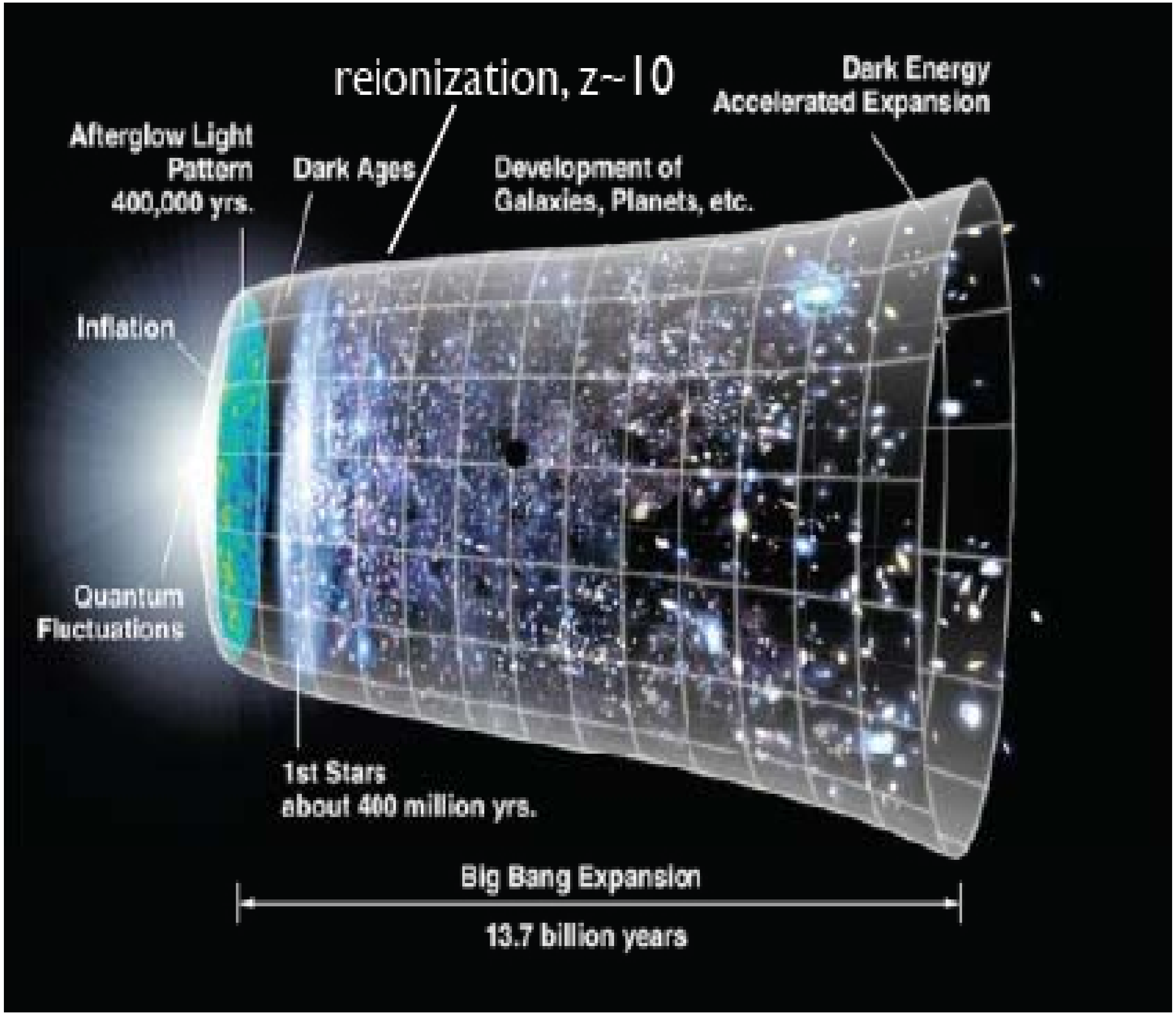

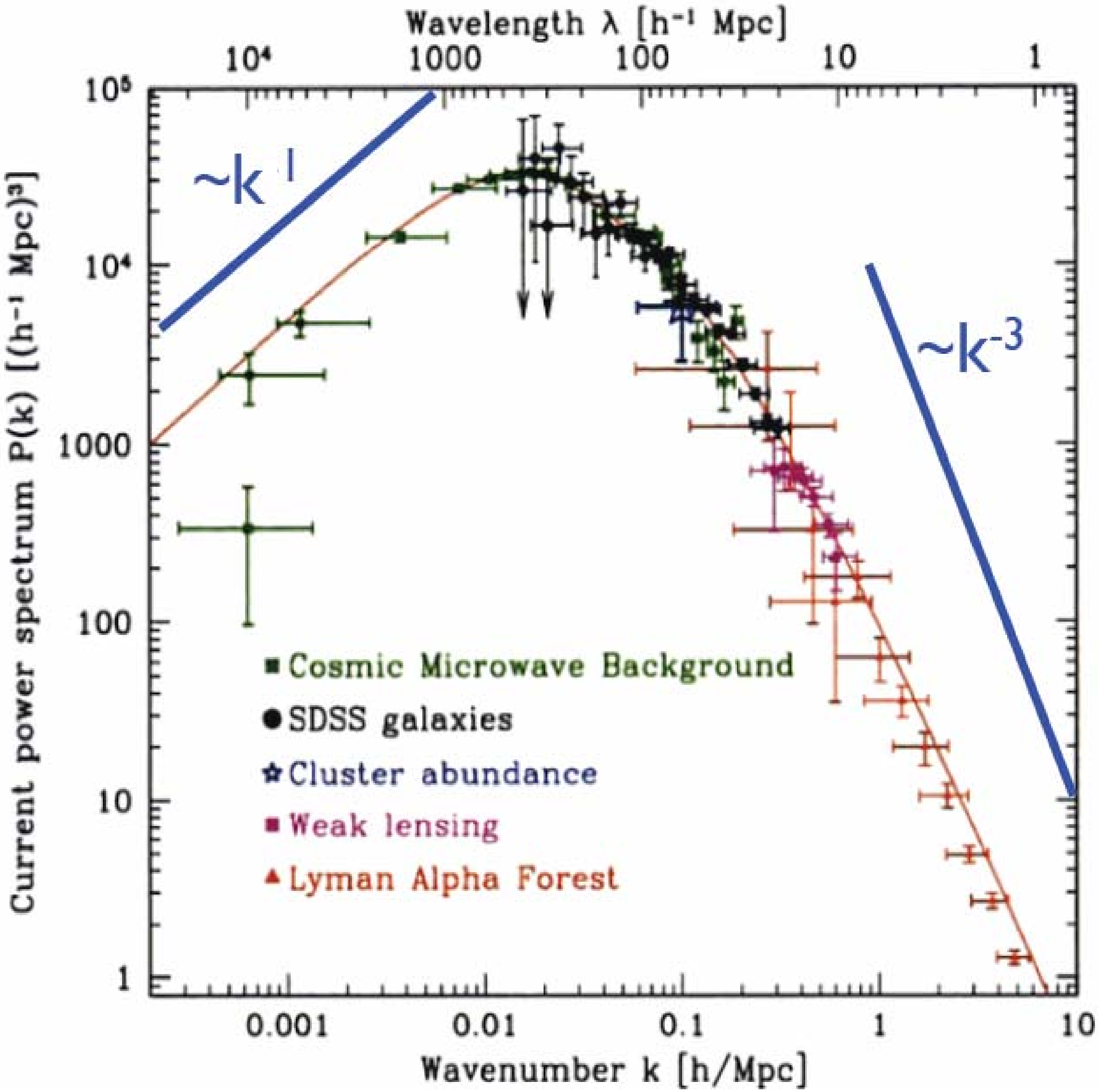

Wavelength λ [h⁻¹ Mpc]
10⁴
1000
100
10
1
10⁵
10⁴
1000
100
10
1
Current power spectrum P(k) [(h⁻¹ Mpc)³]
~k¹
~k⁻³
Cosmic Microwave Background
SDSS galaxies
Cluster abundance
Weak lensing
Lyman Alpha Forest
0.001
0.01
0.1
1
10
Wavenumber k [h/Mpc]

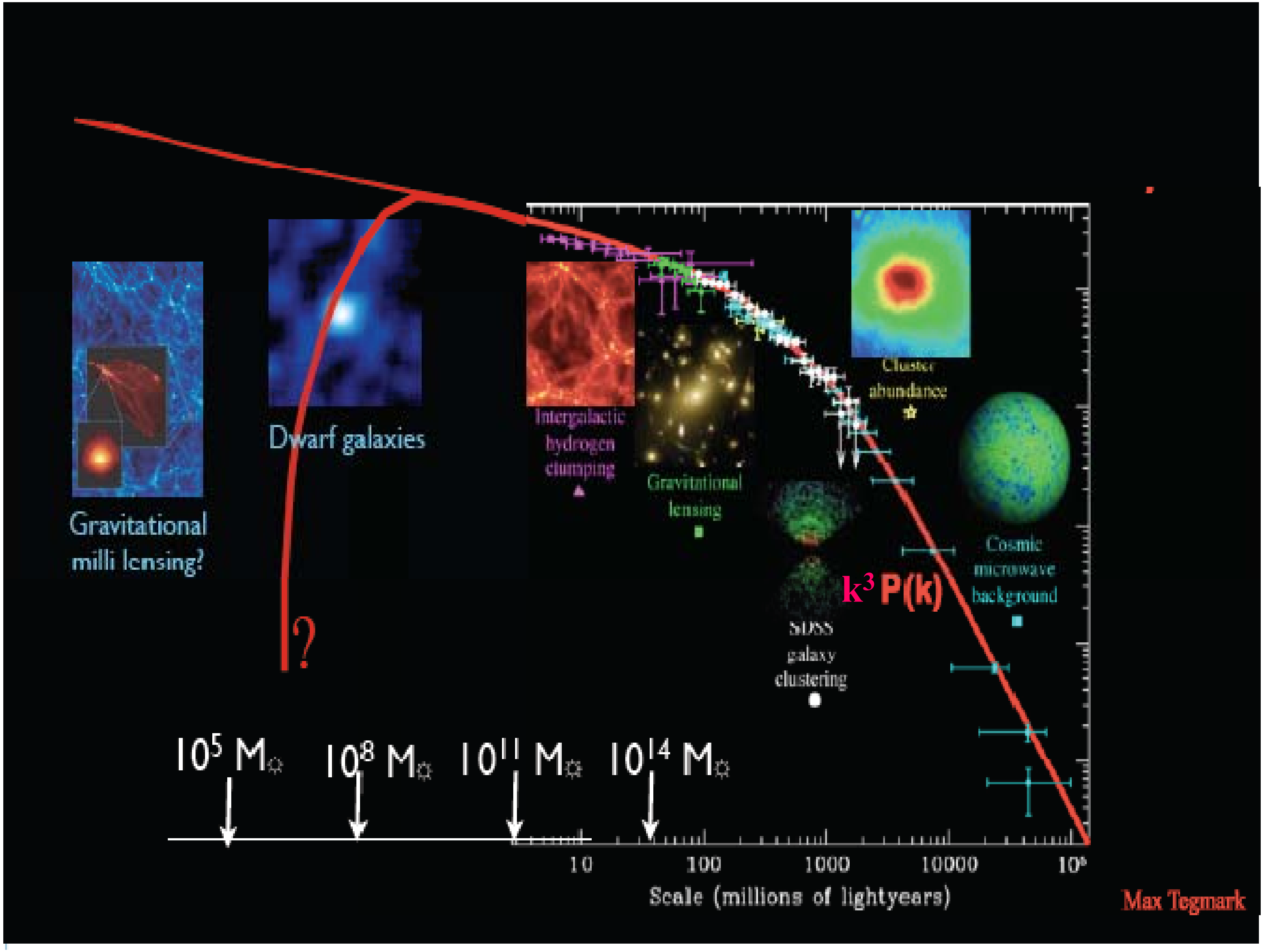

Gravitational
milli lensing?
Dwarf galaxies
Intergalactic
hydrogen
clumping
Gravitational
lensing
Cluster
abundance
Cosmic
microwave
background
SDSS
galaxy
clustering
k³ P(k)
?
10⁵ M☉
10⁸ M☉
10¹¹ M☉
10¹⁴ M☉
10
100
1000
10000
10⁵
Scale (millions of lightyears)
Max Tegmark

WHERE ARE THE MISSING GALACTIC SATELLITES?

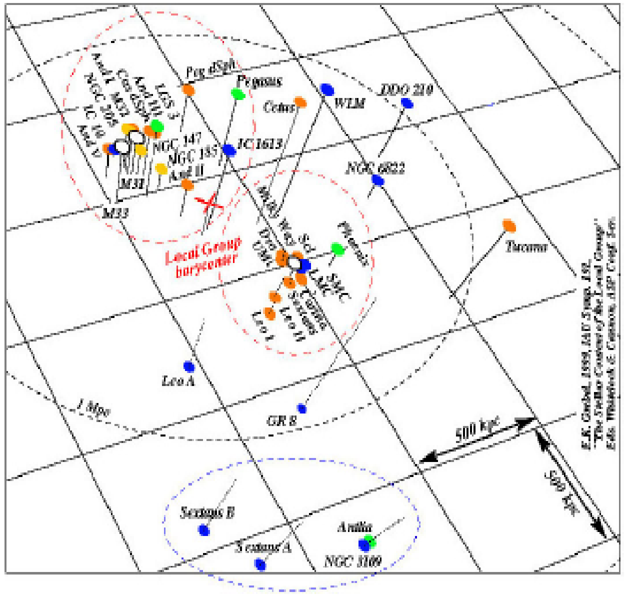

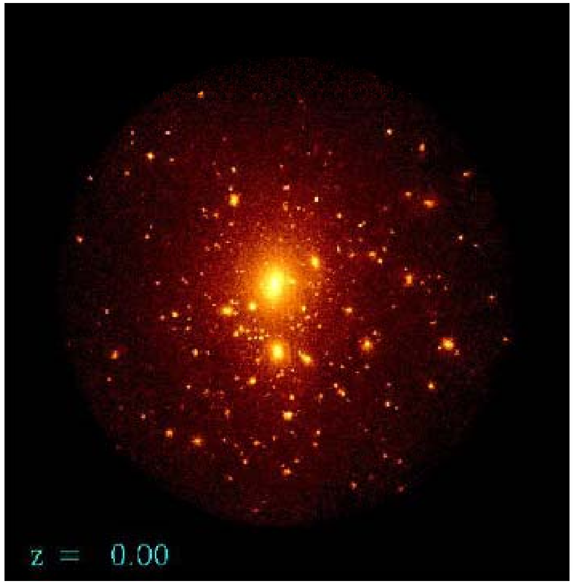

The LCDM model predicts that thousands of dwarf DM haloes should exist in the Local Group while only ~50 are observed.

Klypin et al.,1999, Moore et al.,1999, Madau et al., 2008

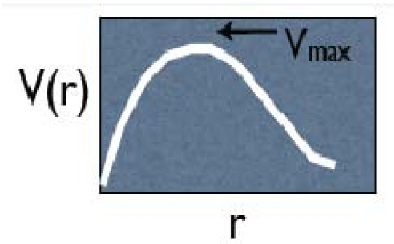

$V(r) = (GM(r)/r)^{1/2}$

count subhalos within virial radius of a simulated M~10^{12} M_{sun} halo

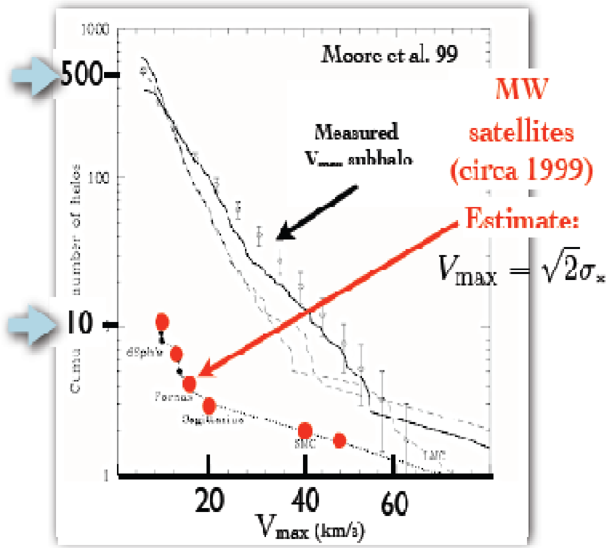

2001

THE VOID PHENOMENON

astro-ph/0101127

P. J. E. PEEBLES

From continuity one might have thought the more likely picture is that gravity has emptied the voids of mass as well as galaxies. This does not happen in the CDM model, however. Simulations show, between the concentrations of large dark mass halos, clumps of mass that seem to be capable of developing into void objects observable as clumps of stars or gas, contrary to what is observed.

2008

THE VOID PHENOMENON EXPLAINED

astro-ph/0804.2475

JEREMY L. TINKER[1] & CHARLIE CONROY[2]

The void phenomenon consists of two observational facts: that voids contain few, if any, low-luminosity galaxies, and that the few void objects tend to have similar properties to the overall galaxy population. The controversial aspect is whether these facts are at odds with the current cosmology. Although the depth of voids and homogeneity of void objects are striking features of the cosmic web, they are readily explainable within the context of ΛCDM, combined with a straightforward model to connect galaxies and dark matter at all luminosities and mass scales.

Anton Tikhonov /SPbSU

Anatoly A. Klypin /NMSU; Stefan Gottloeber /AIP; Gustavo Yepes /UAM

The emptiness of voids in LWDM-model: possibility to escape LCDM-overabundance?

1. LCDM model faces the same overabundance problem, which it had with the number of satellites in the LG: the theory predicts a factor of 10 more haloes as compared with the observed number of dwarf galaxies. (A.V. Tikhonov, A. Klypin, 2008, arXiv:**0807.0924**)

2. Problems faced by CDM-models on Mpc and sub-Mpc scales motivated reconsideration of WDM (**Warm Dark Matter**)-**models** with typical masses of particles $\mathbf{m_X}$ around **1keV** which decouple being still ultra-relativistic.

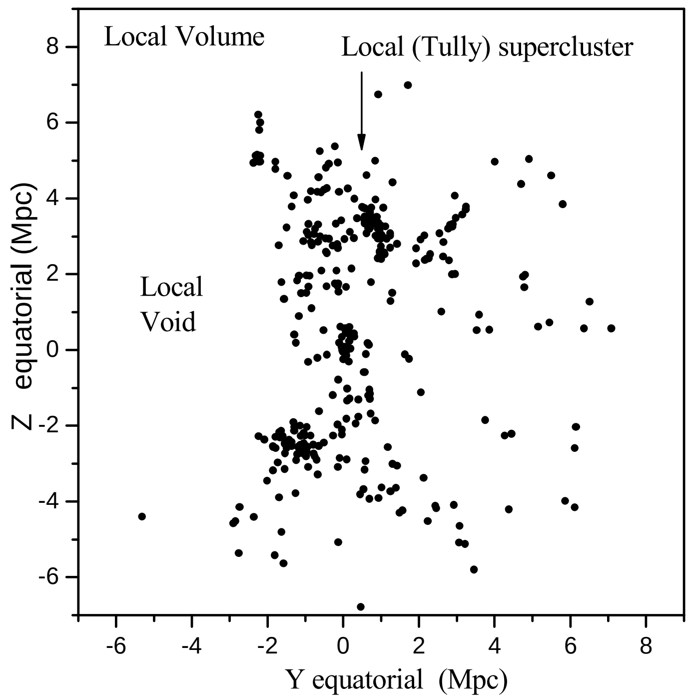

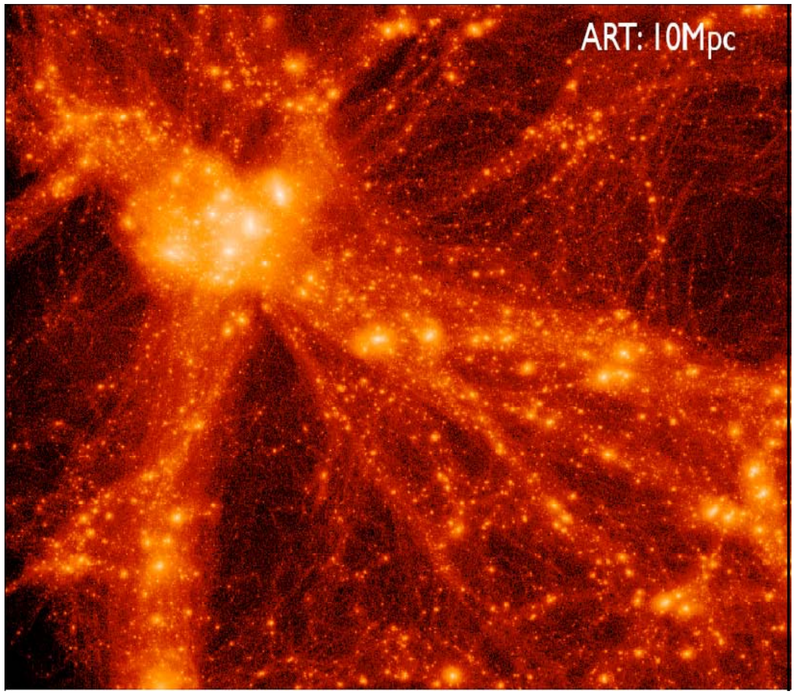

How small can be a galaxy?

Below some mass the haloes are expected to **stop producing galaxies** inside them.
There are different arguments for that:

stellar feedback (Dekel, 1986) or

photoionization (Bullock, 2000)

may play a significant role in **quenching starformation** in **too small haloes**.

For example, (**Loeb, 2008**) made a simple estimation of the limiting circular velocity V_{lim} below which haloes have essentially **no gas infall** due to **increase of Jeans mass** caused by **UV background** at the **epoch of reionization**:

$$V_{lim} = 34 \cdot (T_{IGM} / 1.5 \cdot 10^4\ K)^{1/2}\ km/s,$$

where T_{IGM} is thetemperature of intergalactic medium gas ionized by stars.

(**Hoeft, 2006**) studied formation of dwarf DM haloes in cosmologicalvoid regions using high-resolution hydrodynamic simulations andassuming that **cosmological UV-background photo-evaporates baryons out of haloes of dwarf galaxies**, and thereby limits their cooling and starformation rate.

(**Hoeft, 2006**) give characteristic mass $M_C = 6 \cdot 10^9\ h^{-1} M_{sun}$ below which haloes start to fail accreting gas.

What luminosity a halo or subhalo with given circular velocity *should have* in order to reproduce the observed spectrum of void sizes?

$$V(r) = (GM(r)/r)^{1/2}$$

$$V_c = 20 km/s \ -\ M_{vir} \sim 10^9\ M_o$$

$$V_c = 50 km/s \ -\ M_{vir} \sim 10^{10}\ M_o$$

At the present time, the sample of galaxies with distances less than 10 Mpc numbers about 550 galaxies. For half of them the distances have been measured to an accuracy as high as 8-10% (**Karachentsev et al., 2004**, the average density of luminosity within the radius of 8 Mpc around us exceeds **1.8 - 2.0** times the global luminosity density. Almost the same excess is also seen in the **local HI mass density**. About 2/3 of the LV galaxies belong to the known virialized groups like the LG.

Parameter	M.Way	M31	M81	CenA	M83	IC342	Maffei
D, Mpc	0.01	0.78	3.63	3.66	4.56	3.28	3.01
Nv	18	18	24	29	13	8	8
σ_v,km/s	76	77	91	136	61	54	59
R_p, Mpc	.16	.25	.21	.29	.16	.32	.10
T_{cross}, Gyr	2.1	3.3	2.3	2.2	2.7	5.9	1.8
M_{vir}, 10^{10}	95	84	157	725	86	76	100
L_B, 10^{10}	3.3	6.8	6.1	6.0	2.5	3.2	2.7
M/L, solar	29	12	26	121	34	24	37

Karachentsev et al., 2005

No. 4, 2004 CATALOG OF NEIGHBORING GALAXIES 20

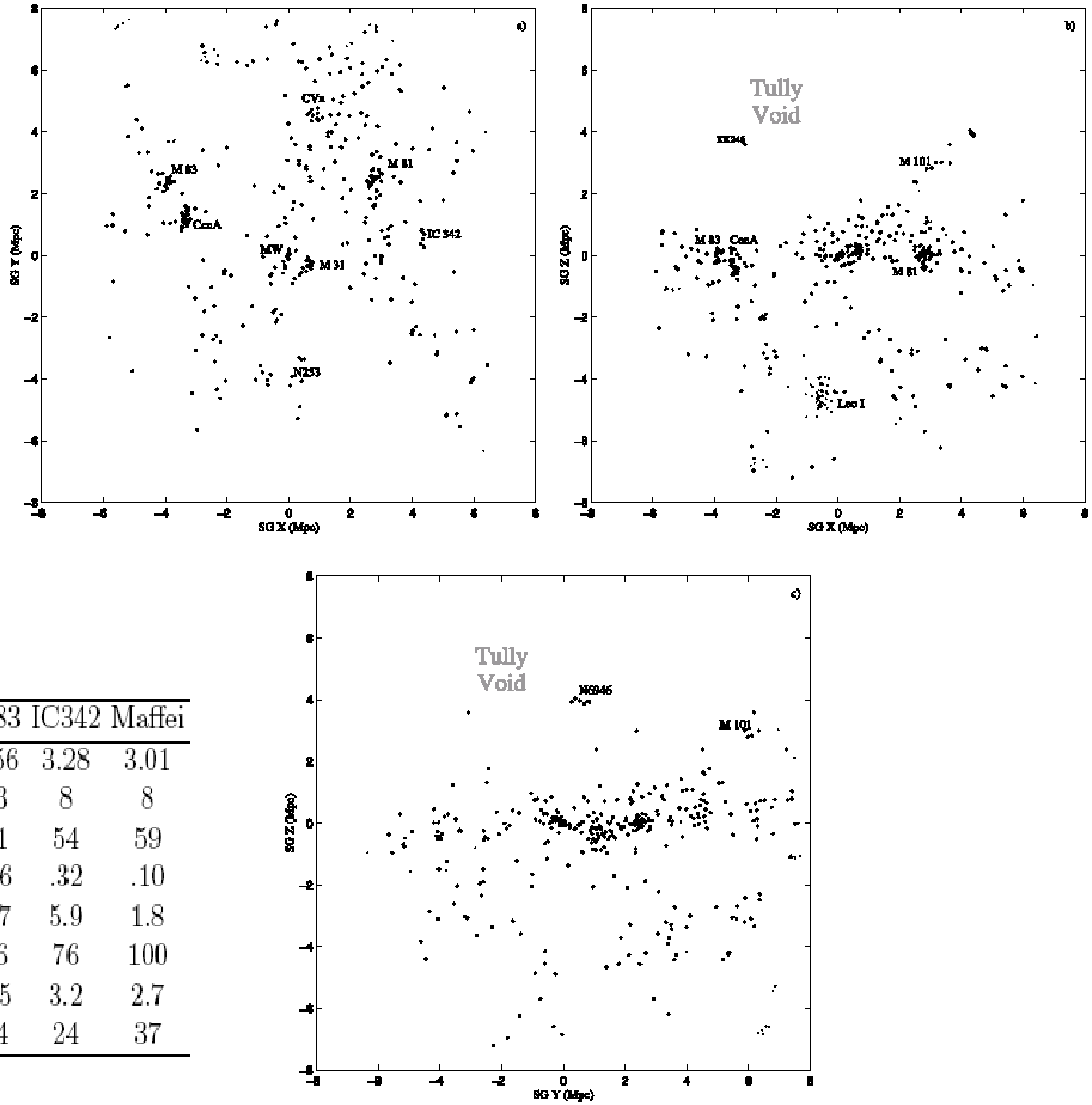

FIG. 5.—Panorama of the LV within a radius of 8 Mpc in Cartesian supergalactic coordinates. Galaxies from Table 1 with $D > 8$ Mpc are shown as small circl
(*a*) SGX-SGY, galaxies projected onto the plane of the Local Supercluster; (*b*) SGX-SGZ, the distribution in *Z* (perpendicular to the plane of the Local Superclust

Void detection algorithm

• **3D grid**.
• **Empty seed sphere** of largest possible radius $\mathbf{R_{seed}}$ is identified.
• **Expansion of seed spheres** by spheres with radius $\mathbf{R_{sph} > 0.9\ R_{seed}}$ and with centers inside already fixed part of a void.
• **Next seed sphere** is determined. Process continues until $R_{seed} > R_{threshold}$.
• **Voids have flexible but still regular shapes and are thick enough** throughout their volumes.
• **Voids are defined to be completely inside** sample boundaries.
(El-Ad & Piran,1997, Gottloeber, 2003)
Then we considered

Cumulative void function ΔV/V(>Rvoid)

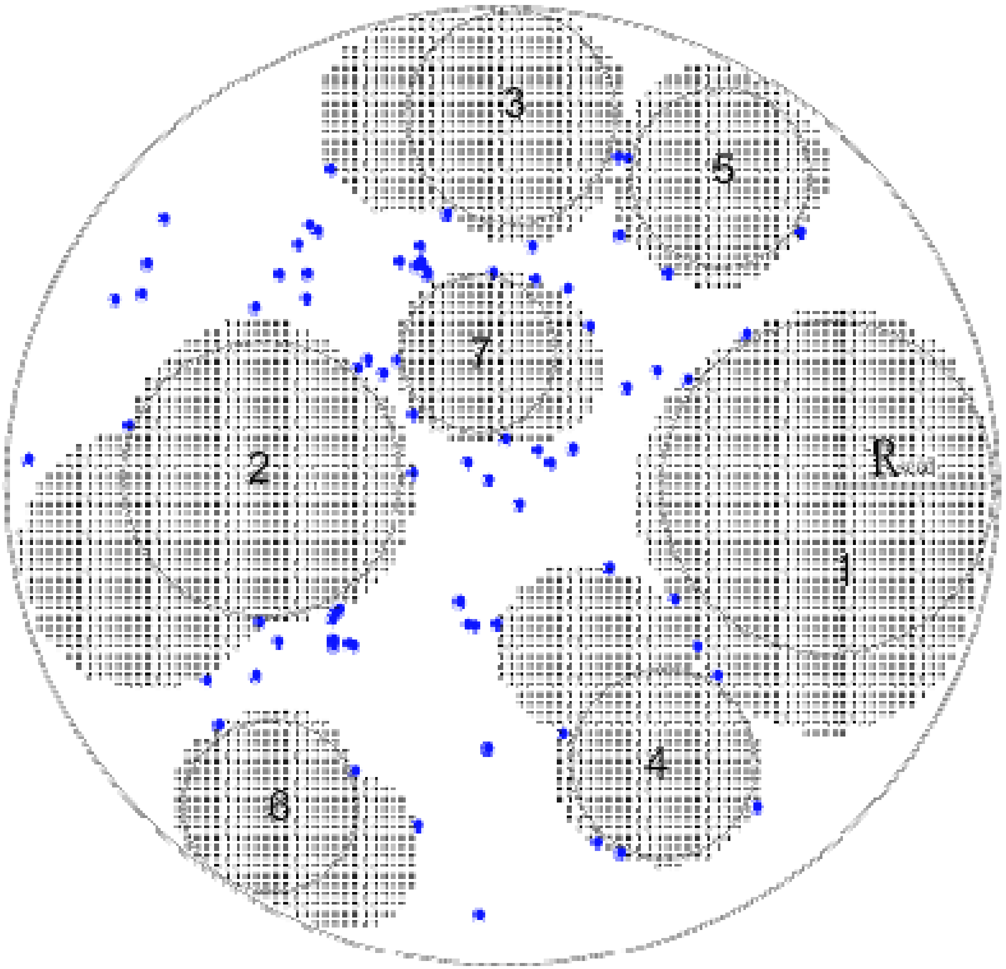

2D-case of point-like distribution. Seed circles and voids growing from them are shown. The numerals indicate the order of identification of voids

Distribution of six largest minivoids within the LV-sphere of radius 7.5 Mpc.

¼ of the Local Volume is occupied by Void in Aquila - front part of the Local (Tully) Void (**Tikhonov & Karachentsev, 2006)**

Luminosity functions of LV galaxies

The volume limited sample is complete for galaxies with abs. magnitudes **M_B < -12 within 8Mpc** radius. Another volume limited sample is **M_B < -10 within 4Mpc**. Karachentsev (2004)noted that luminosity density in LV in **B**-band with respect to the mean in the Universe about **1.8 - 2** times higher.

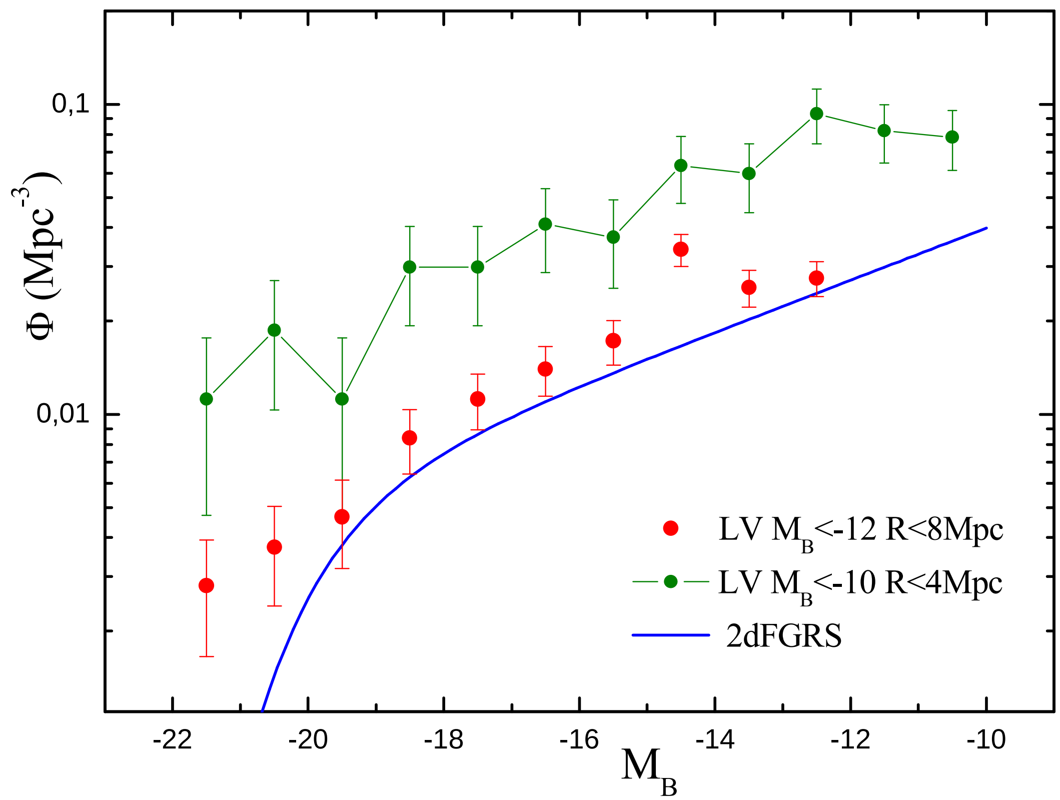

3 SIMULATIONS

We use N-body simulations (1) and (2) done with the Adaptive Refinement Tree code (9) and (3) done with GADGET2 code. As a measure of how large is a halo we typically use the maxumum circular velocity V_c, which is easier to relate to observatons as compared with the virial mass. For reference, halos with $V_c = 50\,\mathrm{km/s}$ have virial mass about $10^{10} M_\odot$ and halos with $V_c = 20\,\mathrm{km/s}$ have virial mass about $10^9 M_\odot$. We use three simulations: (1) (Box80S); spherical region of 14 Mpc inside 80Mpc/h box (mass per particle $3 \times 10^8 h^{-1} M_\odot$) resolved with $5 \times 10^6 h^{-1} M_\odot$ particles; (2) Box160CR 160 Mpc/h aside constrained realization with mass resolution $1.2 \cdot 10^9$; (3) Box64CR 64Mpc/h aside constrained realization with mass resolution $1.6 \cdot 10^7$. The simulations are for a spatially flat cosmological LCDM model with following parameters: (1) $\Omega_0 = 0.3, \Omega_\Lambda = 0.7; \sigma_8 = 0.9; h = 0.7$ (WMAP1 parameters). (2) and (3): $\Omega_0 = 0.24, \Omega_\Lambda = 0.76; \sigma_8 = 0.75; h = 0.73$ (WMAP3 parameters).

We scaled all data (coordinates and masses of halos) to "real" $H_0 = 72$ km/s/Mpc that is the mean value of Hubble flow in the Local Volume and close to the value that comes from WMAP parameters.

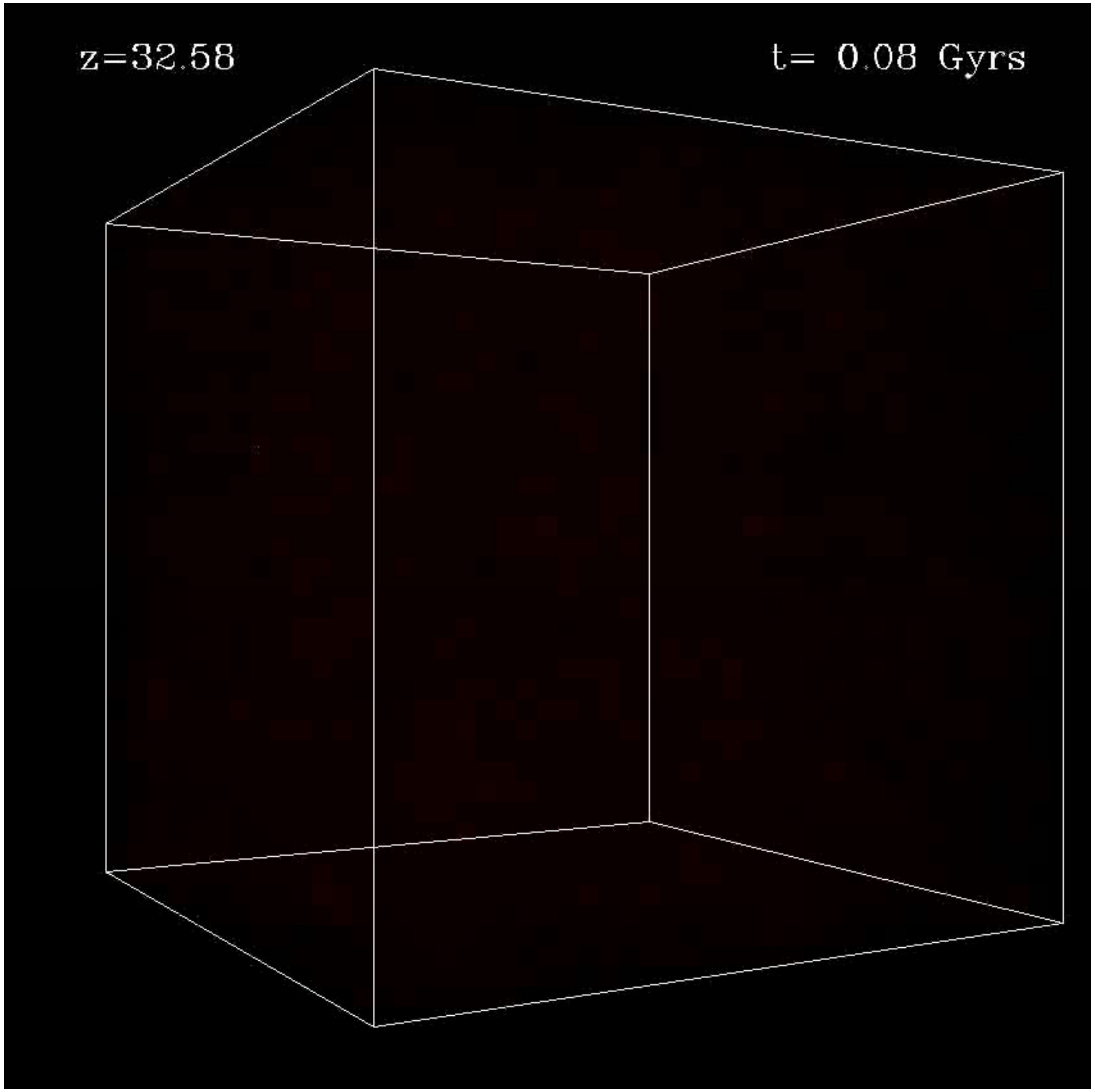

RMS Peculiar Velocity – deviations from the HUBBLE FLOW - σ_H

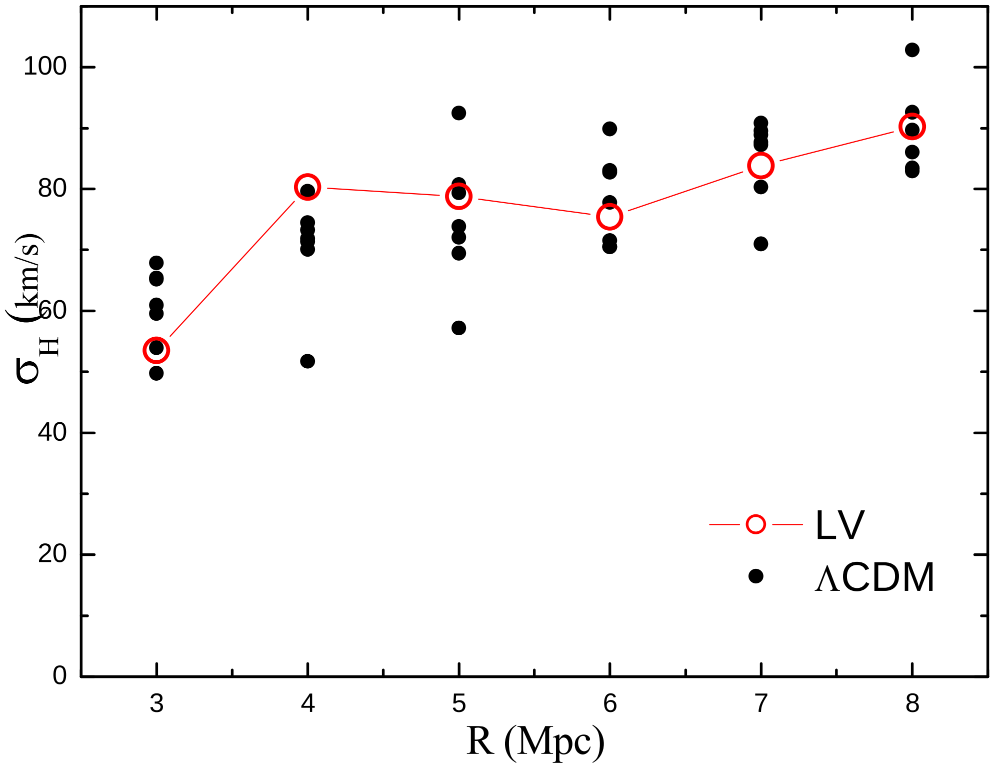

Figure 2. σ_H^{true} with apex and error correction for LV in the volume from 1 Mpc up to R Mpc with σ_H in corresponding volume for 7 model LV-candidates from Box160CR.

Apex: min. of $\sum_{i=1}^{N}(v_i - H_0 \cdot D_i + (Ax \cdot x_i + Ay \cdot y_i + Az \cdot z_i)/D_i)$,

$$\Delta^2\sigma_H = \frac{\alpha^2 \cdot H_0^2 \cdot \sum_{i=1}^{N}(D_i^2)}{N}.$$

Results

Cumulative void function $\Delta V/V(>R_{void}) = V_{voids}(>R_{void})/V_{sample}$, V_{voids} - total volume of voids with $R_{eff} > R_{void}$, V_{sample}- total volume of a sample, $R_{eff} = (3V_{void}/4\pi)^{-1/3}$.

Local Volume

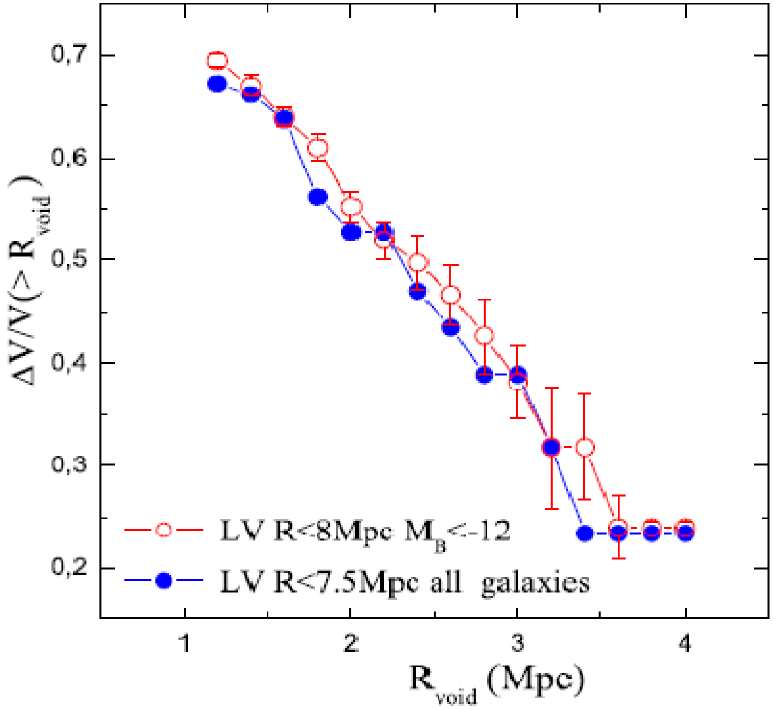

Figure 4. the void function for two observational samples. The full curve with open circles are for a complete volume limited sample with $M_B < -12$ and $R < 8$ Mpc. 1σ errors obtained by Monte Carlo resampling distances from catalog by means of additon gaussian distributed characteristic error of distance measurements. The filled circles are for all observed galaxies inside 7.5 Mpc. Comparison of the samples shows reasonable stability of the void function.

Box64CR $\sigma_8 = 0.75$

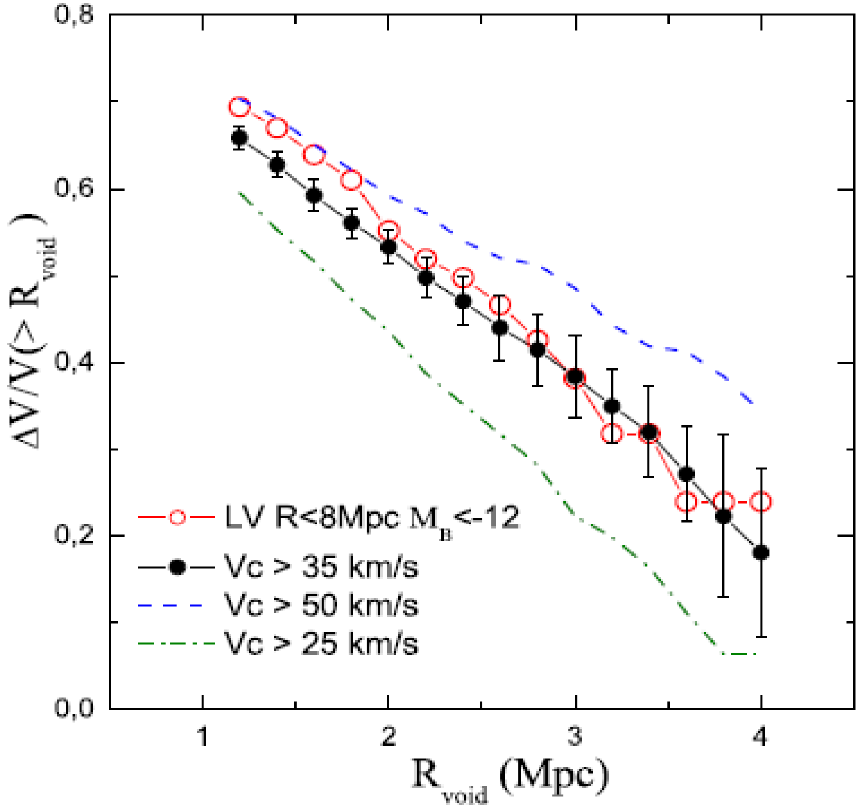

Figure 5. Observational data (the complete sample $M_B < -12$) are compared with the distribution of voids in 14 samples from Box64CR of halos with different limits on halo circular velocity. In this case VF for $V_c = 35\,\mathrm{km/s}$ (shown with 1σ scatter) provides a better fit to observations.

Box160CR $\sigma_8 = 0.75$

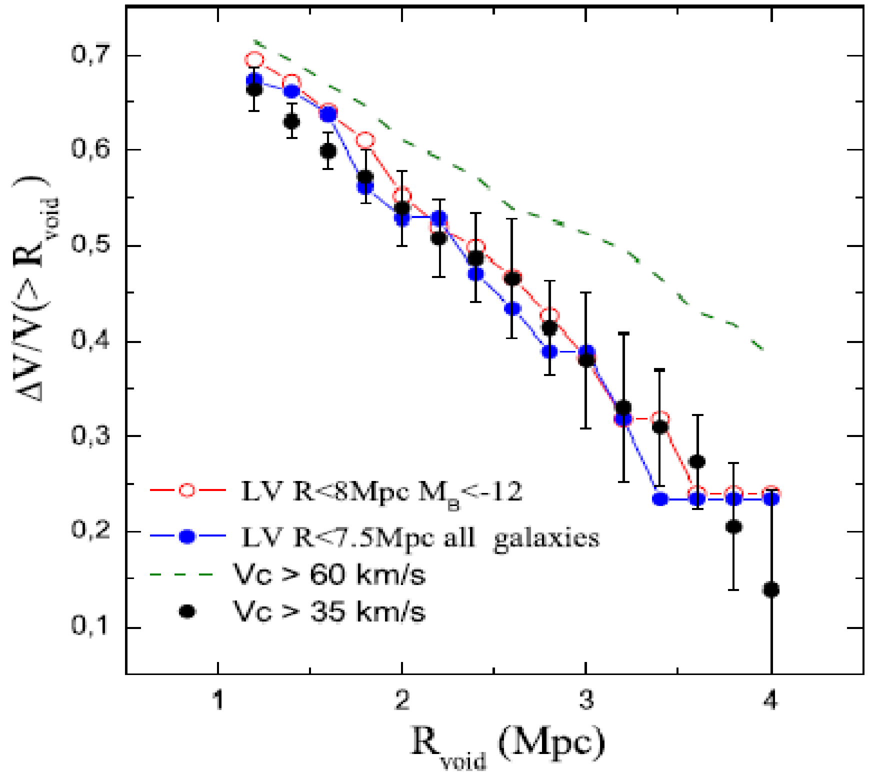

Figure 6. Observational data (the complete sample $M_B < -12$) are compared with the distribution of voids in 7 samples from Box160CR of halos with different limits on halo circular velocity. CVF for $V_c = 35\,\mathrm{km/s}$ (shown with 1σ scatter) provides a remarkably good fit to observations. Because of resolution here we can not plot curves below observational VF

LCDM- Overabandance

Isolated dIrr $V_{\rm rot} = W_{50}/2\sqrt{1-(b/a)^2}$

Table 4. Properties of isolated dwarf galaxies with $M_B = -11.8 - 13.2$

Name	M_B	axial ratio	W_{50}	V_{rot}	Distance
E349-031,SDIG	-12.10	0.82	20.0	17.5	3.21
KKH5	-12.27	0.62	37.0	23.6	4.26
KKH6	-12.38	0.60	31.0	19.4	3.73
KK16	-12.65	0.37	24.0	12.9	5.40
KKH18	-12.39	0.57	34.0	20.7	4.43
KKH34,Mai13	-12.30	0.56	24.0	14.5	4.61
E489-56,KK54	-13.07	0.53	33.8	19.9	4.99
KKH46	-11.93	0.86	25.0	24.5	5.70
U5186	-12.98	0.23	42.0	21.6	6.90
E321-014	-12.70	0.43	39.8	22.0	3.19
KK144	12.50	0.33	44.0	23.3	6.30
E443-09,KK170	-12.03	0.75	29.0	21.9	5.78
KK182,Cen6	-11.89	0.60	16.0	10.0	5.78
DDO181,U8651	-12.97	0.57	42	23.7	3.02
DDO183,U8760	-13.13	0.32	30.0	15.8	3.18
HIPASS1351-47	-11.88	0.60	38.8	24.2	5.65

In terms of TF-relation

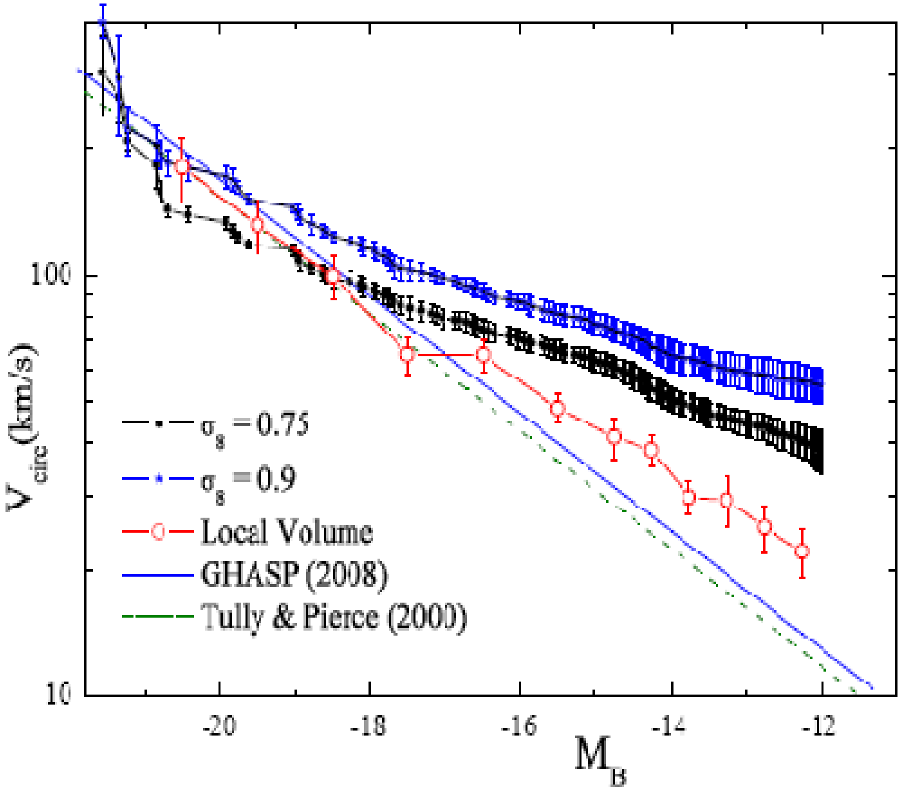

Dwarf Galaxies

dIrr Camelopardalis B; D=2.2Mpc; $M_B = -10.9$

$V_{rot} \sim 10$ km s^{-1}

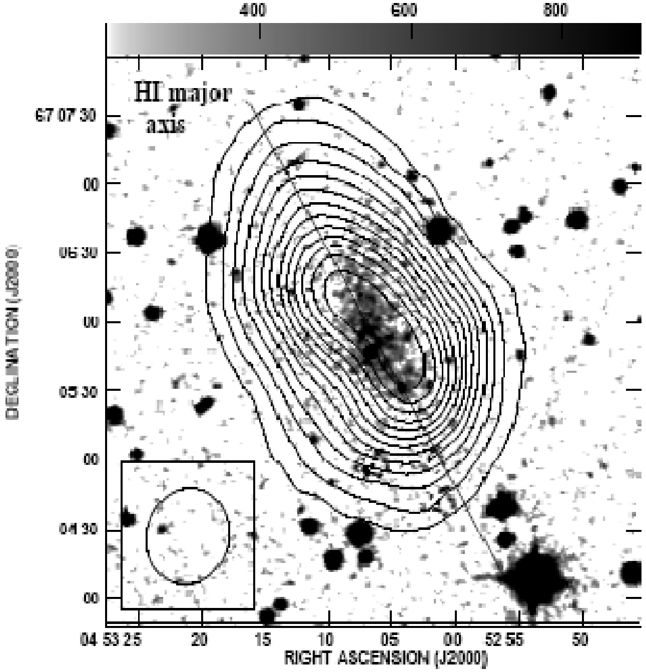

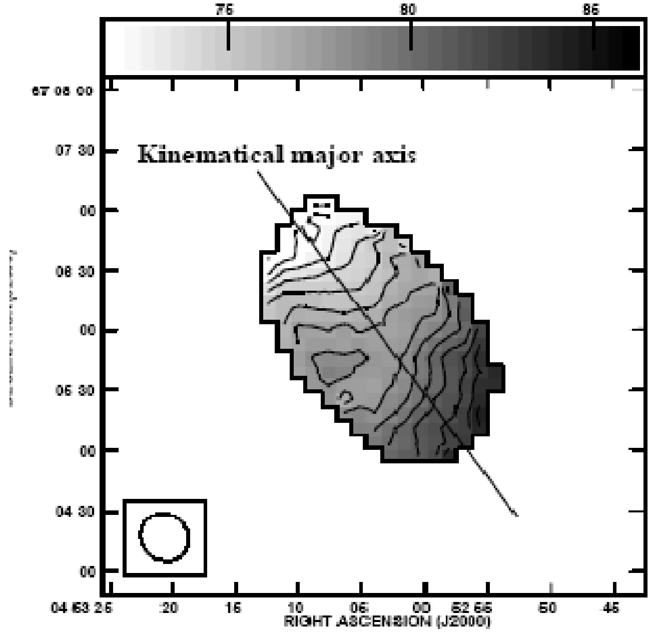

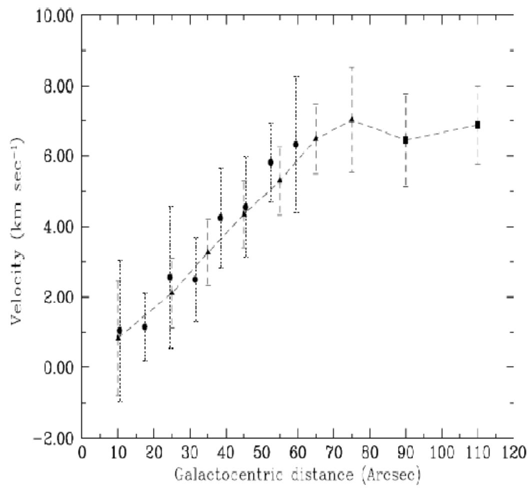

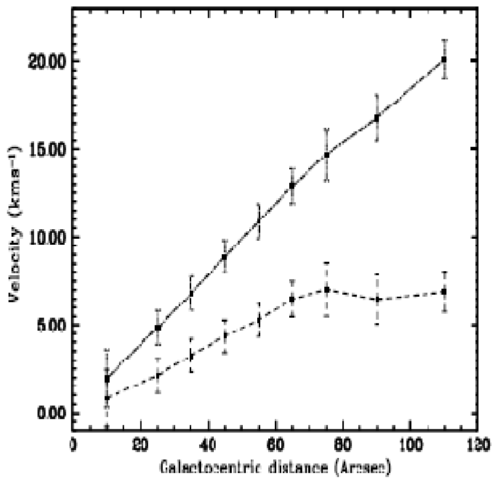

dIrr CGCG 269-049 M_B=−12.46 D=3.4Mpc

$V_{rot}\sin(i) \leq 8$ km s^{-1}

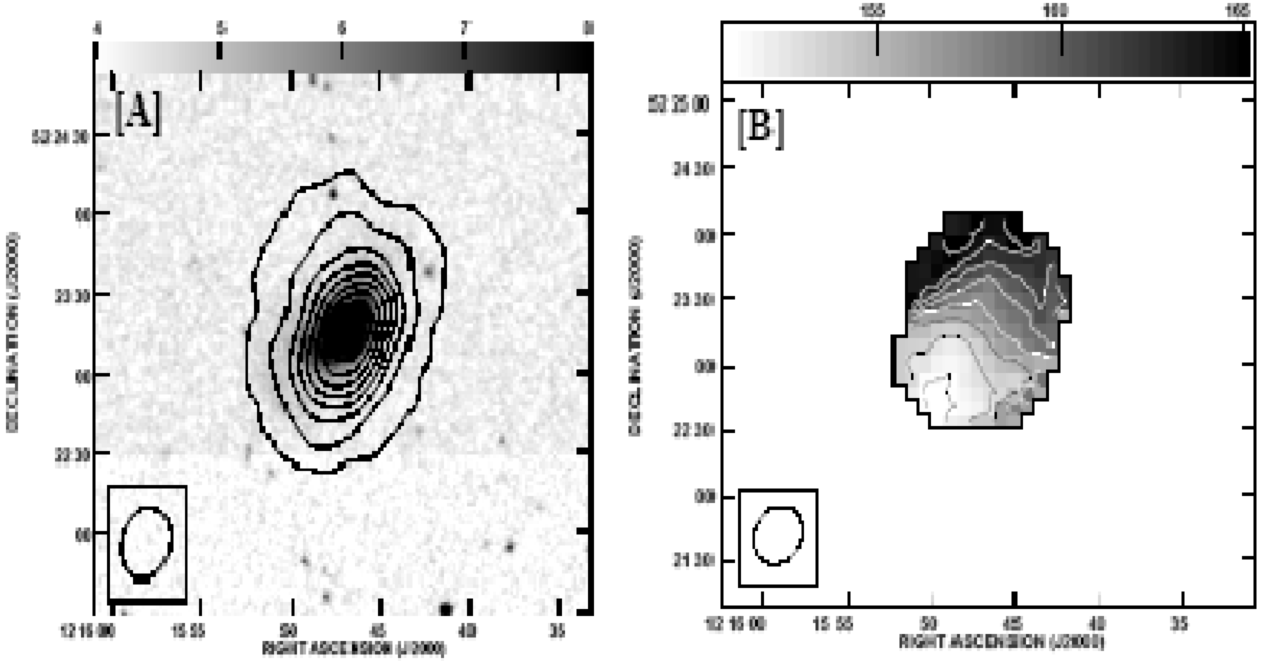

Figure 5. [A] The B band optical DSS image of CGCG 269-049 (greyscales) with the GMRT $28'' \times 24''$ resolution integrated HI emission map (contours) overlayed. The contour levels are 0.08, 1.12, 2.18, 3.23, 4.28, 5.33, 6.39, 7.44, 8.49 and 9.55 $\times 10^{20}$ atoms cm^{-2}. [B] The HI velocity field for galaxy at $28'' \times 24''$ resolution. The contours are in the steps of 2.0 km s^{-1} and range from 151.0 km s^{-1} to 165.0 km s^{-1}.

WDM-paradigm m_X =1keV

Box 64h^{-1}Mpc, h=0.72 WDM and CDM WMAP3

Initial conditions

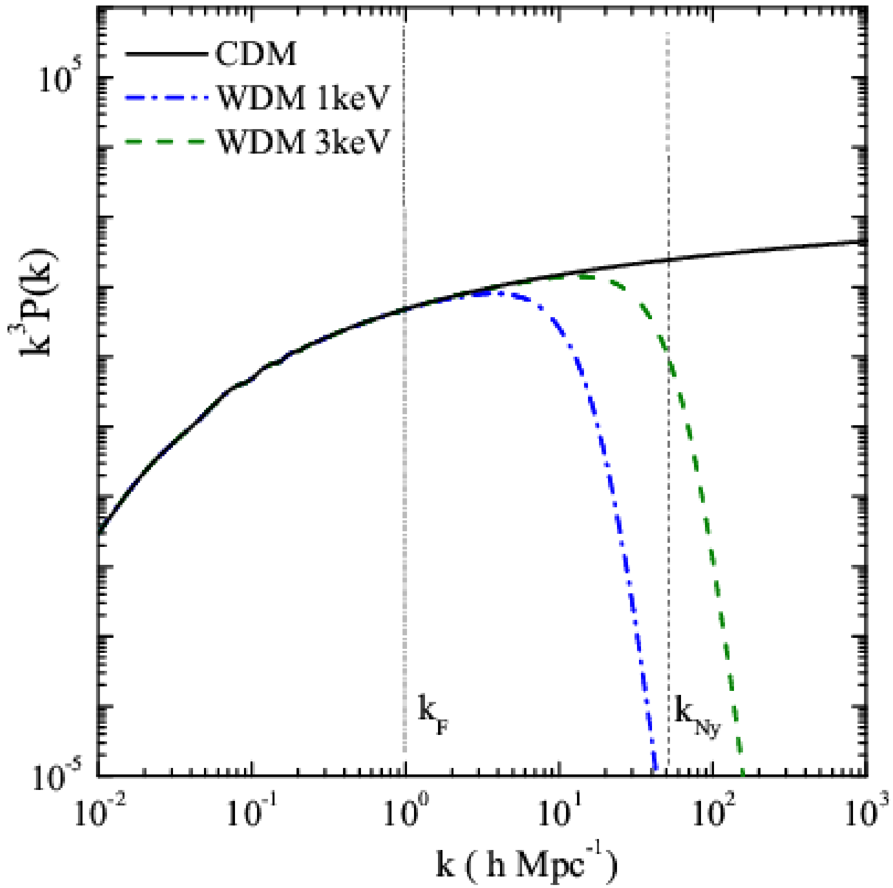

Resulting haloes

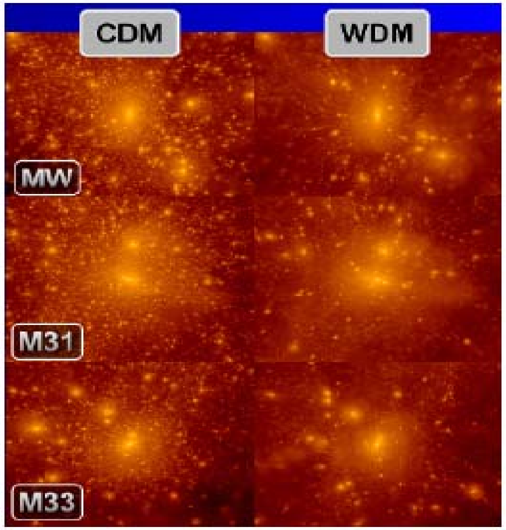

Arman Khalatyan

WDM

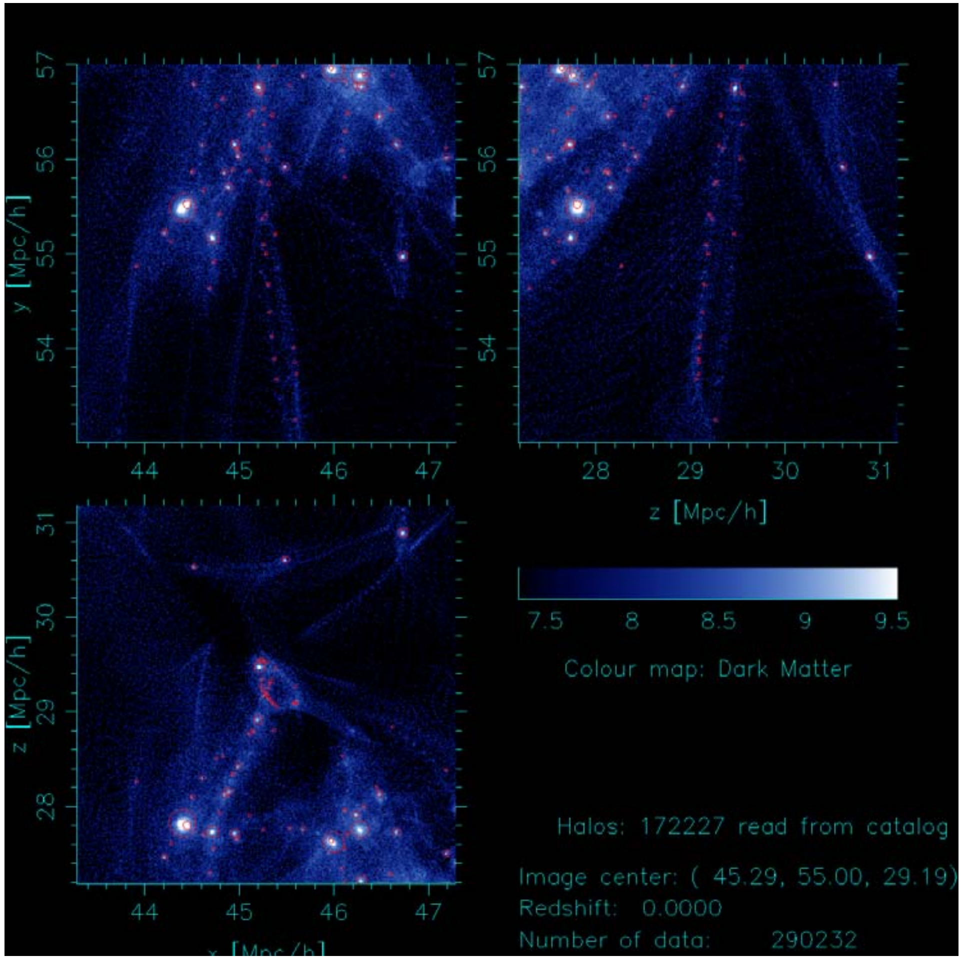

CDM

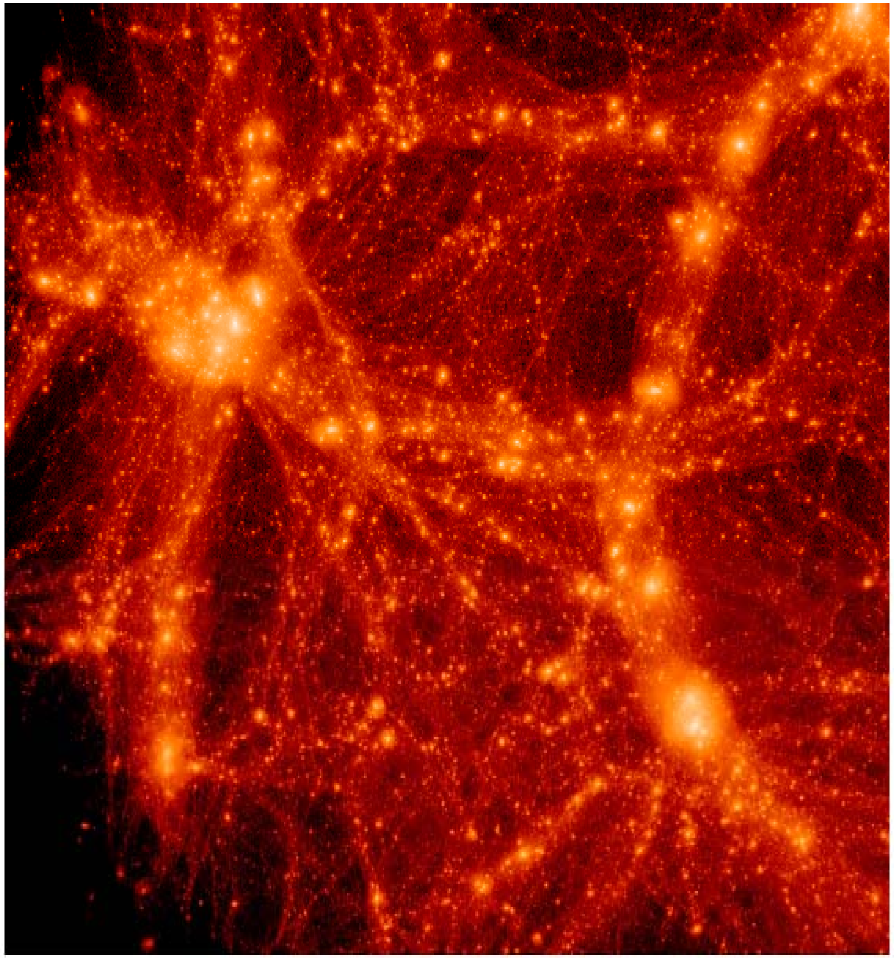

WDM-like simlations (with P(k)-truncation suffer by fake-haloes:

Appeared via spurious fragmentation of filaments

Wang&White, 2007; Klypin, 2008

Halos in voids

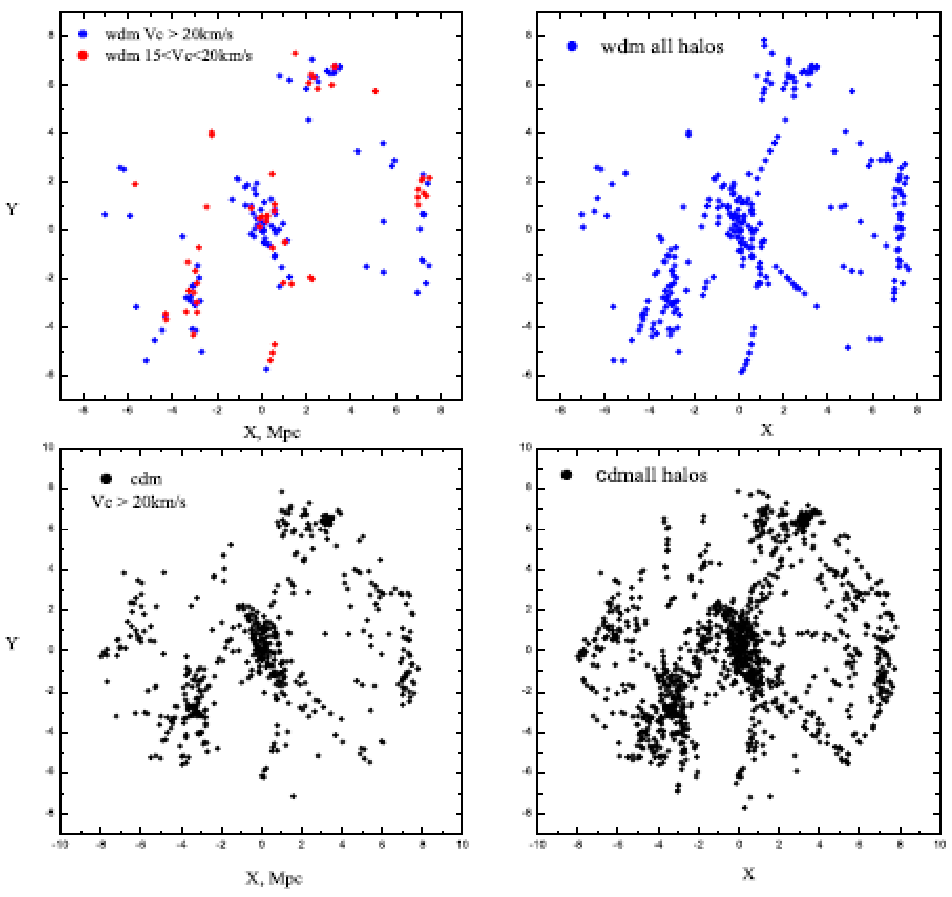

WDM

CDM

Figure 4. Distribution of halos in the one of our "LV-candidate" from CDM64and WDM64catalogs. The upper panels shows wdm-halos: with $V_c \geqslant 20\,\mathrm{km/s}$ (red circles on upper left plot indicate halos with $15 < V_c < 20\,\mathrm{km/s}$) and all halos in the slice throw the sample center 4 Mpc thick. Regular chains of small fake-halos are clearly seen. Distribution of corresponding cdm-halos is shown on lower panel

Void-functions

WDM

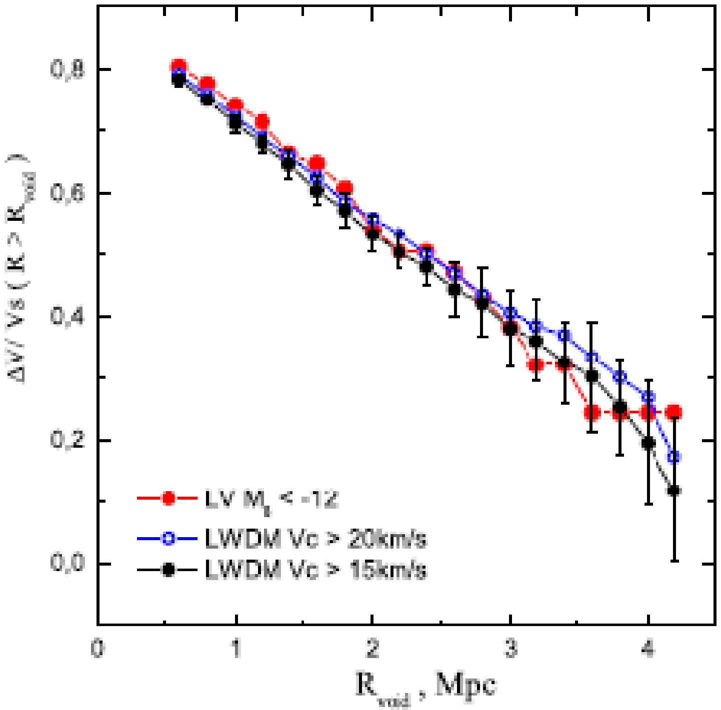

V^{lim} = 15-20 km/s

CDM

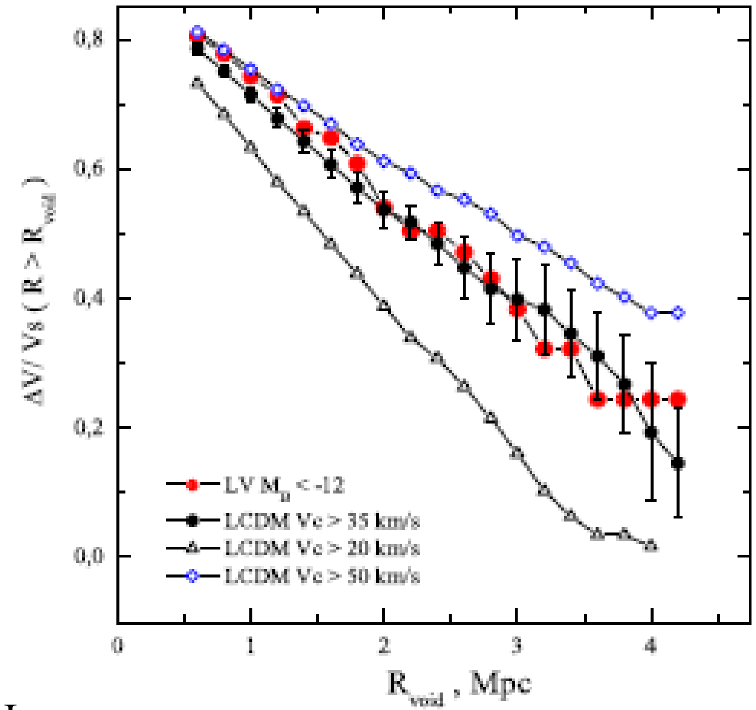

V^{lim} = 35 km/s

σ_H

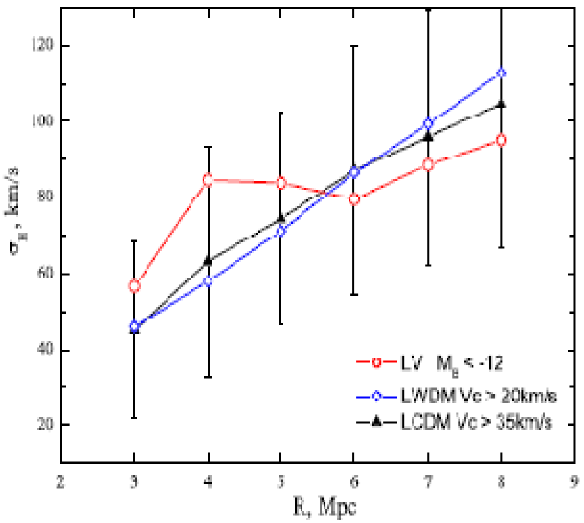

Conclusions

Problem:

The LCDM model faces the same overabundance problem, which it had with the number of satellites in the LG: the theory predicts a factor of ten more halos as compared with the observed number of dwarf galaxies.

Solutions:

1. Thousands of **dSph** in the field to find out

2. Halo $\mathbf{V_c \sim 2V_{rot}}$:dwarf galaxies are hosted by significantly more massive haloes.

3. Dwarf formation was **suppressed** by e.g. UV- background

4. L**WDM**-**models (P(k) - truncation)** $m_X \sim 1$keV